Regional variations in the European Neolithic dispersal: the role of the coastlines

Daniel A. Henderson[1], Andrew W. Baggaley[2], Anvar Shukurov[1], Richard J. Boys[1], Graeme R. Sarson[1] & Andrew Golightly[1]

The mechanisms by which agriculture spread across Europe in the Neolithic, and the speed at which it happened, have long been debated. Attempts to quantify the process by constructing spatio-temporal models have given a diversity of results. In this paper, a new approach to the problem of modelling is advanced. Data from over 300 Neolithic sites from Asia Minor and Europe are used to produce a global picture of the emergence of farming across Europe which also allows for variable local conditions. Particular attention is paid to coastal enhancement: the more rapid advance of the Neolithic along coasts and rivers, as compared with inland or terrestrial domains. The key outcome of this model is hence to confirm the importance of waterways and coastal mobilities in the spread of farming in the early Neolithic, and to establish the extent to which this importance varied regionally.

Keywords: Europe, Asia Minor, Neolithic dispersal, modelling, waterways, propagating population front, wave of advance

Supplementary material is published online at http://antiquity.ac.uk/projgall/henderson342

Method

Introduction

Agriculture was introduced into Europe during the last epoch of the Stone Age, the Neolithic. Agricultural technologies spread across the continent from about 7000 to 4000 BC. This was a systematic process. The change from foraging to farming first occurred in the Levant and then dispersed across a few thousand kilometres to France, Iberia and Britain (Clark 1965; Ammerman & Cavalli-Sforza 1971; Gkiasta *et al*. 2003) at a speed that remained remarkably constant at 1.0–1.3km/yr on average, despite the wide diversity in the topographic, climatic, soil and water systems and conditions. The stability of the average propagation speed strongly suggests a common, fundamental mechanism for the spread, which was identified as a propagating front of a population (or a relevant cultural trait) that conforms to the logistic growth law and disperses via random movements of the individuals and cultural traits (see Czárán (1998) for the general concepts of population dynamics and Fort (2009) and Steele (2009) for reviews of their application to prehistory). Similarly, the Neolithic spread across

[1] *School of Mathematics & Statistics, Newcastle University, Newcastle upon Tyne NE1 7RU, UK (Email: daniel.henderson@ncl.ac.uk; anvar.shukurov@ncl.ac.uk; richard.boys@ncl.ac.uk; g.r.sarson@ncl.ac.uk; andrew.golightly@ncl.ac.uk)*

[2] *School of Mathematics & Statistics, University of Glasgow, Glasgow G12 8QW, UK (Email: andrew.baggaley@glasgow.ac.uk)*

Asia to the Indus Valley; Gangal *et al.* (2014) estimate the speed of the Neolithic dispersal in Asia as 0.5–0.8km/yr.

Although the *average* speed of the Neolithic dispersal in Europe remained the same across the continent, it varied locally. Rowley-Conwy (2011) emphasises that the spread of agriculture involved rapid, sporadic local movements. The most-discussed examples are the spread of the Linearbandkeramik (LBK) along the Danube–Rhine river system at a speed of 4–6km/yr (Ammerman & Cavalli-Sforza 1971; Dolukhanov *et al.* 2005)—although see the discussion below—and the propagation of the Impressed Ware (Cardial) culture along the western Mediterranean coast at 10km/yr or a slightly lower speed (Zilhão 2001, 2003). Bocquet-Appel *et al.* (2009, 2012) identify a number of fine spatio-temporal structures in the Neolithic dispersal in Europe.

We stress that the concept of a propagating population front (or a wave of advance), as applied to characterise the global picture, is fully consistent with the sporadic and irregular nature of local movements (including small 'leap-frogs'; see the later discussion). The shape of the front modelled here is quite irregular in response to the local environment, but our model is still firmly in the category of a wave of advance model. Furthermore, both population migration and cultural transmission exhibit similar trends, and our arguments and results apply irrespective of whether or not the Neolithic dispersal was dominated by human migrations, as was plausibly the case.

The importance of waterways in the spread of the Neolithic has been well established and documented (Davison *et al.* 2006; Rowley-Conwy 2011). The most striking examples are the Danube–Rhine river system and the northern Mediterranean coastline. The North Sea coast, however, apparently was not used for maritime colonisation, even though Rowley-Conwy argues that spread by boat up the coast brought the Neolithic to Scandinavia, which required "longer open-water voyages than in the Cardial or LBK" (Rowley-Conwy 2011: S442). The Neolithic transition in the British Isles and Ireland obviously required maritime travel and Collard *et al.* (2010) suggest that it is best modelled by two distinct centres of settlement, associated with separate arrivals in south-west England and in west-central Scotland. Price (2003), Isern and Fort (2010, 2012) and Bocquet-Appel *et al.* (2012) attribute the slower spread of the Neolithic from the LBK area to the North Sea coast to a higher population density of Mesolithic foragers in the north. However, this does not explain the apparent lack of any relative acceleration of the spread along the North Sea coast whenever the Neolithic reached it.

The local variations in the direction and speed of the dispersal are of obvious importance as they may help us to understand the response of Neolithic farmers to the environment and, by exclusion, to identify those individual dispersal events driven by more exceptional instances of human volition. Before such complex questions can be addressed, however, one needs to identify reliably such discernible local events and their parameters; for example, the local variations in the speed and direction of propagation. ^{14}C age determinations offer a suitable starting point for such investigations (Bocquet-Appel *et al.* 2009, 2012).

Locally enhanced dispersal can affect the global pattern of the spread of farming, as illustrated by Rowley-Conwy (2011: fig. 1). For example, the emergence of the Epicardial to the north and north-west of the Mediterranean coast was clearly facilitated by the accelerated spread of the Cardial along the coastline. Davison *et al.* (2006) demonstrate, with mathematical modelling, this effect and the similar role of the rapid spread of the LBK along the Danube–Rhine corridor in the emergence of the Neolithic further west. The global consequences of the local events significantly affect the interpretation of the ^{14}C (or any other) evidence. For instance, apart from fitting the ^{14}C dates in a given region (LBK areas, for example) with any model, one should ensure that the later dates in other regions (in France, for example) are consistent with the properties inferred for the local event. In other words, reliable identification of local dispersal events should involve (and be consistent with) the global data.

In this paper, we suggest an approach to this problem based on a combination of mathematical modelling and statistical analysis of ^{14}C data. We use a model of a population front propagating at a variable speed controlled by the local conditions (mainly the topography) with the model parameters fitted to achieve good agreement with ^{14}C data from 302 early Neolithic sites in Asia Minor and Europe. Details of the ^{14}C data set used, the population front model and the statistical techniques used can be found in Baggaley *et al.* (2012a & b), and are summarised in the online supplementary material. Here we describe the model only briefly and focus on its implications.

Model of the Neolithic dispersal

The main goal of this paper is to quantify the spread of the Neolithic population front along the European waterways in finer detail than in earlier studies of this kind. Our population front model includes a systematic, global propagation affected by the local topography and augmented with a localised additional spread along major waterways. The waterway speed is a fitted parameter of the model and it is allowed to be different in different regions.

A population front propagating in an inhomogeneous environment

To keep tractable the number of the model parameters, we include five regions with potentially distinct waterway speeds: 1) the eastern Mediterranean; 2) the western Mediterranean and the western coast of Iberia; 3) Northern Europe, the Atlantic coast of France and the northern coast of Iberia; 4) the Danube–Rhine river system, and 5) the Black Sea coast. The choice of these specific regions is discussed below. These regions are shown in Figure 1 together with the ^{14}C-dated sites used in the analysis. Being aware of the global consequences of the local variations, the model parameters are fitted using the ^{14}C age determinations in the whole of the area modelled.

Our population front model tracks the time-evolving location of the wave front. It does this by tracking a set of suitably separated points on the front, and allowing them to propagate with the local front velocity determined by the local environment. In brief, we model the population front by propagating each of the points that define it at the local velocity represented by three terms, $\boldsymbol{U} + \boldsymbol{V}_{\mathrm{R}} + \boldsymbol{V}_{\mathrm{C}}$. Here $\boldsymbol{U} = \boldsymbol{U}_0 F(a, \phi)$ is the global propagation velocity. In population dynamics models based on the reaction-diffusion equation, U_0 depends on the population growth rate γ and a measure of its mobility ν as $U_0 = |\boldsymbol{U}_0| = 2\sqrt{\nu\gamma}$ (Steele 2009). Earlier analyses of the ^{14}C data yield $U_0 \approx 1$km/yr (Gkiasta *et al.* 2003), consistent with $\gamma = 1/(50\text{yr})$ and $\nu = 13\text{km}^2/\text{yr}$. In our model,

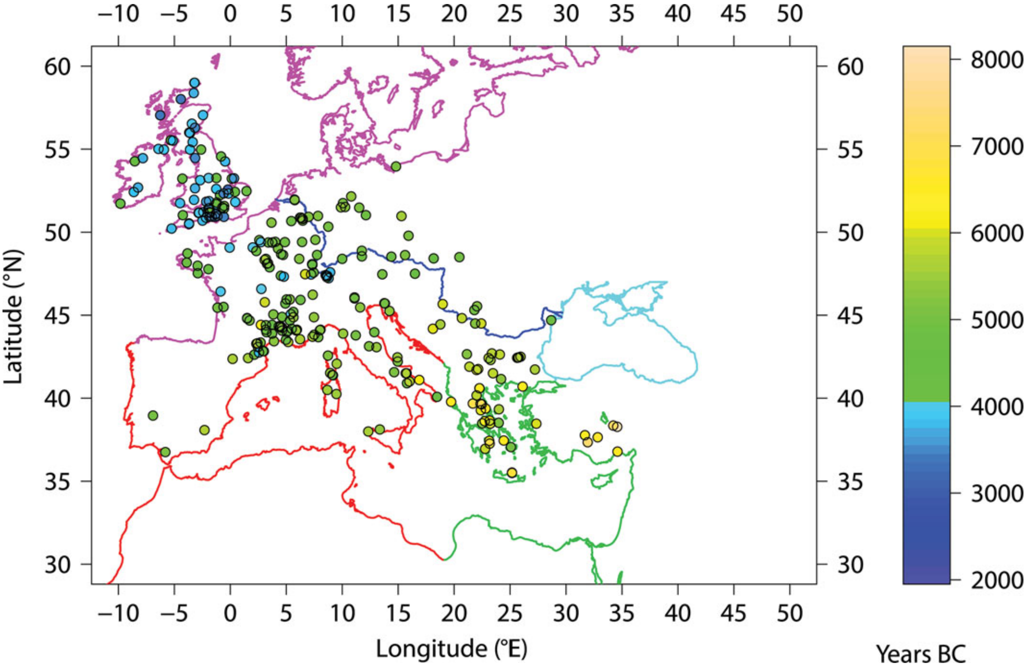

Figure 1. The location of the 302 Early Neolithic sites used in the analysis, with colour representing their age. The ^{14}C data and their interpretation are described in detail by Baggaley et al. *(2012b). The distinct coastal and river regions used in the model are also shown: eastern Mediterranean (green); western Mediterranean and the west-Atlantic coast of Iberia (red); Northern Europe, the Atlantic coast of France and the northern coast of Iberia (purple); the Black Sea (light blue); and the Danube–Rhine system (dark blue).*

U_0 is one of the fitted parameters. The factor $F(a, \phi)$ introduces the dependence on the altitude a and latitude ϕ; the form of F is such that the magnitude of $\boldsymbol{U}$ slowly decreases northwards (reducing F by 12% as ϕ varies from 40° N to 50° N) and is truncated at altitudes exceeding $a = 1$km and in the sea. The direction of $\boldsymbol{U}$ is always at a right angle to the local front, so that it has different directions at different positions as the front becomes curved, e.g. in response to topographic features such as mountain ranges (introduced via the variable a, the altitude). The other velocities, $\boldsymbol{V}_{\mathrm{R}}$ and $\boldsymbol{V}_{\mathrm{C}}$, add further local variation, but these are confined to 30km-wide corridors around the Danube and Rhine and the sea coast, respectively. The velocities $\boldsymbol{V}_{\mathrm{R}}$ and $\boldsymbol{V}_{\mathrm{C}}$ are directed parallel to the corresponding river path or coastline; the coastal velocity $\boldsymbol{V}_{\mathrm{C}}$ is allowed to have different values in the regions specified above, denoted $\boldsymbol{V}_i$, with $i = 1,2,3,4$. The magnitudes of $\boldsymbol{V}_{\mathrm{R}}$ and $\boldsymbol{V}_i$ are the other fitted parameters of the wavefront model. Given these components of the velocity, the position of the front is evolved from a compact source in the Levant. The form of the population front, as introduced here, strongly depends on the local topography and latitude, as well as on the waterways, so that it can (and does) have a complicated shape. As shown in Figure 2, it is not the perfectly circular front erroneously envisaged by many as a feature inherent to the wave of advance model. A perfectly regular population front only occurs in perfectly homogeneous environments, often favoured by mathematicians but

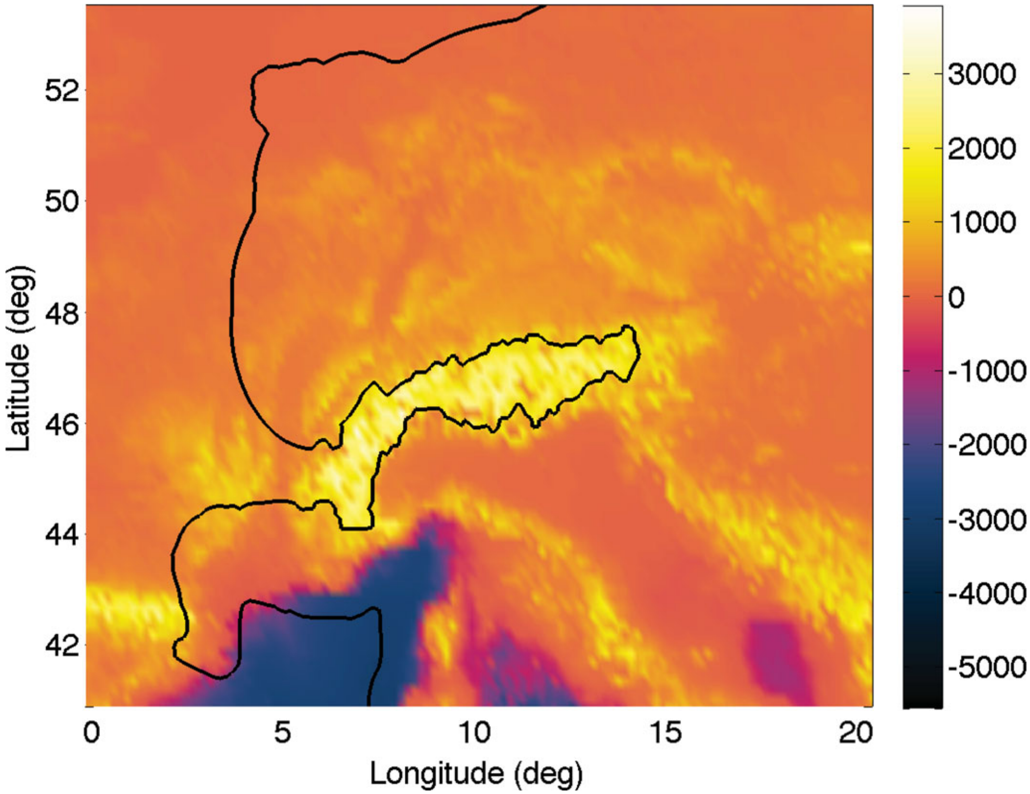

Figure 2. A section of the population front, obtained in the simulations described in the text, is shown by the black line. Note the irregular shape of the front that results from the dependence of its propagation velocity on altitude (colour coded, in metres). The front is shown moving around the Alps (in the centre of the frame) and is clearly faster along the western Mediterranean coastline (the lower left corner). The model allows coastal sea travel as the population mobility decreases gradually away from a coastline into the sea at an exponential length scale of 10km. In addition, there is a slight 'tongue' in the upper Rhine area (top left) due to the enhanced spread along the river path.

utterly unrealistic. Further details of the propagating front model are described in the online supplementary material and by Baggaley *et al.* (2012b).

Statistical modelling

With the model introduced above, we calculate when the front reaches the sites shown in Figure 1 and compare them with the Neolithic arrival times at those sites obtained from their ^{14}C ages. The model parameters listed in Table 1 are then varied, as described below, to obtain parameter values that provide plausible agreement between the observed and calculated first arrival times. This gives us a range of models or 'plausible histories' of the wave of advance that are consistent with the data, rather than just a single best-fitting model.

The Bayesian approach to statistical inference (Bernardo & Smith 1994) provides a natural framework with which to quantify our beliefs about the model parameters. Adopting a Bayesian approach, we express initial beliefs about likely parameter values via a prior probability distribution for each parameter. Our choice of the prior distributions

Table 1. Model parameters with summaries of their prior and posterior probability distributions. HN(a, b^2) denotes a half-normal distribution; that is, a normal distribution with mean a and variance b^2 that has been truncated to take values greater than or equal to a; LN(c, d^2) denotes a log-normal distribution: if $X \sim$ LN(c, d^2), then $\log X$ is normally distributed with mean c and variance d^2; finally, Gamma(e, f) denotes a gamma distribution with mean e/f and variance e/f^2. We used the MCMC scheme to generate 800 000 samples from the posterior probability distribution of the parameters. Using sampling importance resampling (SIR; Rubin 1988), we have confirmed that the results are robust to small changes in the prior distributions.

Notation	Description (units)	Prior distribution	Prior mean (SD)	Prior 95% range	Posterior mean (SD)	Posterior 95% range
U_0	Background front speed (km/yr)	LN(0.5, 0.71^2)	2.1 (1.7)	0.4–6.6	0.96 (0.04)	0.9–1.0
V_R	Additional speed along Danube–Rhine (km/yr)	HN(0, 20^2)	16 (12)	0.6–44.8	1.8 (1.4)	0.06–5.29
Additional coastal speeds						
V_1	Eastern Mediterranean (km/yr)	HN(0, 5^2)	4 (3)	0.2–11.2	0.7 (0.2)	0.2–1.0
V_2	Western Mediterranean (km/yr)	HN(0, 5^2)	4 (3)	0.2–11.2	11.1 (1.0)	9.3–13.1
V_3	Northern Europe (km/yr)	HN(0, 5^2)	4 (3)	0.2–11.2	0.9 (0.7)	0.03–2.76
V_4	Black Sea (km/yr)	HN(0, 5^2)	4 (3)	0.2–11.2	1.0 (0.7)	0.06–2.62
σ	Global error (yr)	$\sigma^{-2} \sim$ Gamma(2.2, 10^6)	825 (391)	411–1803	577 (24)	533–625

allows freedom in their subsequent modification towards the final (posterior) probability distributions informed by the observed ^{14}C dates. The prior distributions are specified for each model parameter in the third column of Table 1. These beliefs are updated via Bayes' Theorem to obtain a posterior probability distribution for the model parameters that quantifies our beliefs refined after incorporating the ^{14}C data.

The posterior probability distributions do not have any simple form because of the complex dependence of the front behaviour on the model parameters. As in Baggaley *et al.* (2012b, we use Markov chain Monte Carlo (MCMC) methods (Gammerman & Lopes 2006) to draw specific parameter values from their posterior distributions. Each sampled set of parameters represents a competing model of the spread of the Neolithic. The match between the data and the model is quantified in terms of the associated error σ; the larger σ, the greater the average deviation of the wavefront model from the data (see the online supplementary material for details of this parameter). Having repeated the sampling many times, we obtain the posterior (final) probability distribution of the parameters consistent with the ^{14}C data within the accuracy given by the posterior value of σ, which is of order 600 yr. Table 1 contains, in the last four columns, estimates of the parameters (posterior mean), their uncertainty (standard deviations) and their 95% confidence intervals, together with the corresponding estimates for σ. We note that the posterior mean values do not give the global best fit to the data due to the asymmetry of the posterior probability distributions, but they are nevertheless representative of a model that provides a good overall match to the data. Given the many sources of uncertainty and variability surrounding the data and the mathematical model, we would not want to place too much importance on a single explanation of the European Neolithic expansion, such as that provided by the posterior mean or mode. The posterior intervals provide a summary of the variability in the parameter values that are consistent with the data.

The Bayesian approach allows us to determine parameter values that provide good global agreement with the ^{14}C data, together with parameter uncertainties and their cross-correlations. The latter provide us with an opportunity to control the construction of the model by identifying extraneous and mutually dependent parameters (if any). Further details of our statistical model are described in the online supplementary material.

Results: the different roles of different waterways

The background, globally averaged speed of the population front U_0 is determined confidently as $U_0 = 0.96 \pm 0.04$km/yr, which is consistent with earlier results (Ammerman & Cavalli-Sforza 1971; Gkiasta *et al.* 2003).

We find, with various degrees of confidence, evidence for an enhancement in the spread of the Neolithic along European coastlines, with the magnitude of the additional speed estimated as 0.7±0.2, 11±1, 0.9±0.7 and 1.0±0.7km/yr along the eastern Mediterranean, western Mediterranean, Northern European and Black Sea coastlines respectively.

The enhancement along the Mediterranean coast is the most significant. There is strong evidence of an acceleration by about 10km/yr along its western part. This confirms the estimate of Zilhão (2001). Ammerman and Cavalli-Sforza (1971) found an acceleration by 0.7km/yr for the Balkans, in perfect agreement with our result for the eastern Mediterranean despite the fact that the two regions do not fully overlap and we only focus on the coastlines here. This degree of agreement between the two estimates may indicate the importance of maritime colonisation in the Balkans.

For the coastline of Northern Europe, we find the most probable additional speed of around 0.9km/yr, but with a comparable error of 0.7km/yr. The posterior probability distribution of this parameter is wide and asymmetric with the 95% confidence interval of 0.03–2.76km/yr. This suggests that a modest acceleration along the North Sea coast is likely, but it is clearly much weaker than that in the south-west of Europe.

Any effect of the Black Sea coast appears to be similarly weak, although the small number of data points used in this region do not strongly constrain this effect.

The enhancement of the spread in the Danube–Rhine corridor, $V_R = 1.8 \pm 1.4$km/yr, is marginally, yet noticeably, smaller than the estimate of 3–5km/yr (adding with the background 1km/yr to give the total of 4–6km/yr) derived from local analyses of the LBK spread in that area (Dolukhanov *et al.* 2005). This may be in part because our current model effectively gives an averaged enhancement along the whole length of the two rivers, rather than just in the region of the LBK sites used in the papers cited above. This is discussed further below.

The posterior correlations between the model parameters are mostly fairly low, except for a few notable exceptions. The background rate of spread U_0 and the river velocity V_R are negatively correlated: naturally, if U_0 is lower, V_R must be larger to fit the data adequately. Similarly, there is a slight negative correlation between U_0 and the speed enhancement in the eastern Mediterranean, V_1. We also find evidence of a fairly complex dependence between the speed enhancements in the east and west of the Mediterranean, V_1 and V_2. Some degree of negative correlation between these two parameters is not surprising given the geographical proximity of, and causal connection between, the two regions.

Discussion

Our results confirm several of the conclusions of earlier studies. Accelerated spread of the Neolithic along the western Mediterranean coast is confirmed. We have also found firm evidence for a modest acceleration of the Neolithic dispersal in the eastern Mediterranean. This coastal acceleration helps to explain the relatively rapid spread from Anatolia into Europe, as observed by Bocquet-Appel *et al.* (2012); those authors identified this as a response to the cool, dry climatic event of 6250 BC. To achieve good fits to the data, our model also assumes a relatively late starting date of 6570 BC for the dispersal from the Levant; in this respect, our model agrees well with that of Fort *et al.* (2012), whose best fit was obtained using explicit coastal steps of order 100–200km, and leaving the Levant only after the Pre-Pottery Neolithic B/C phase, at 7050 BC.

Our results also suggest that a relatively weak acceleration along the North Sea coast is possible, but this cannot be pinned down accurately with the data and model used. The spread in this region of Northern Europe is of considerable interest; Bocquet-Appel *et al.* (2012), among others, have suggested a slow-down in the spread here, associated with greater resistance from local Mesolithic populations. Investigation of this possibility in our model would require additional data; while newer data for this region are available—e.g.

as compiled in Hinz *et al.* (2012)—there is considerable advantage for the present work in retaining the dataset used in Baggaley *et al.* (2012a & b), as this allows a clear analysis of the effect of introducing variable coastal speeds, which the use of a different dataset would obscure.

As with any modelling, the results cannot be any better than the model itself. The relevance of our results certainly depends strongly on the relevance of the model used. For example, the estimate of the additional propagation speed along the North Sea coast can be affected by our choice of the region where the component V_3 is applied. At present, this region includes the French Atlantic coast and the northern coast of Iberia, even though there are no reasons to expect any significant acceleration in these areas, especially in the general southward spread towards western Iberia. This could have biased our estimate of V_3 towards lower values. The pronounced tail towards larger values in the posterior probability distribution of V_3 suggests that this might be the case. Further work should investigate the effects of different choices for the regions of coastlines, but this should be done in combination with additions to our dataset, most notably in Iberia and in the North Sea region, where our current data is rather sparse. Without these additions, our model will be quite insensitive to the precise location of the boundary between the regions of V_2 and V_3. However, as noted above, there are good reasons to retain the existing dataset in the present work.

Our results support an enhanced spread in the Danube–Rhine corridor. The modal value $V_R = 1.8$km/yr is noticeably larger than the corresponding value from Baggaley *et al.* (2012b, $V_R = 1.0$km/yr; this confirms that allowing different coastal enhancements in different regions is affecting our model globally, and allowing more meaningful fits to the non-coastal parameters. Nevertheless, this enhancement remains weaker than the 3–5km/yr required to explain the rapid spread of the LBK suggested by Ammerman and Cavalli-Sforza (1971) and Dolukhanov *et al.* (2005). The reason for this discrepancy is not quite clear. On the one hand, the value of 3–5km/yr may be an overestimate as it neglects the possible effects of this acceleration beyond the Danube–Rhine corridor. If this is the case, our estimate is more reliable. On the other hand, the construction of our model could have affected the value of V_R inferred: with the spread along the western Mediterranean and French Atlantic coasts accelerated by $V_2 = 11$km/yr and $V_3 = 1$km/yr, respectively, less acceleration along the Danube and Rhine is required to fit the data at the continental scale. The fact that the 95% confidence interval of V_R obtained here extends to about 5km/yr may be an indication of this. It is also worth noting, however, that earlier local analyses (Dolukhanov *et al.* 2005) did not attempt to model the spatio-temporal spread continuously, as our propagating front model does. Within the constraints of the current model, a slower average speed may give the best overall fit to all the local data; an alternative model (e.g. involving discrete long distance moves) might allow for more rapid spread to the west of the LBK region. Here we should also note that the analysis of Bocquet-Appel *et al.* (2012), based on a kriged fit to a more extensive radiocarbon dataset, obtained a mean spread of only 0.8km/yr for sites associated with the LBK culture. Intriguingly, however, the isochrone maps presented in Bocquet-Appel *et al.* (2012) do suggest a relatively rapid spread in the Danube and upper Rhine areas, with a slow-down in the lower Rhine area. This was interpreted as a reasonable rate of spread for the intensive agriculture adopted by the LBK culture, in contrast to the more extensive agriculture adopted by the western Cardial cultures in the western Mediterranean, whose faster spread might plausibly be explained by the agricultural intensity. The spreads in both these regions are certainly interesting phenomena that warrant further study.

Our wavefront-based modelling—and similarly with modelling based on the continuous reaction-diffusion (Fisher–Kolmogorov–Petrovsky–Piskunov) equation—assumes a spatially continuous spread. In addition to incremental, very short-range movements, the spread of a population (or cultural trait) may involve discrete, longer-distance travel events (which may be directed and systematic, or random). It is useful here to distinguish between two types of the latter: relatively smaller events, of less than 100 kilometres, which we here call leap-frogs; and relatively larger events, which we will here call Lévy flights. Models like those discussed here are intended to describe the spread over large distances, and they implicitly incorporate leap-frogs into their specification of the appropriate diffusivities and river/coastal velocities. Diffusion via leap-frog events does ultimately produce an essentially continuous spread when viewed on larger spatial scales.

Spread via persistent, preferentially directed leap-frogs would mathematically be modelled as an anisotropic diffusion, which is conceptually somewhat different from a continuous directed acceleration, as would be mathematically modelled as advection. Within our current model, either effect acting along any particular coastline would, however, result in an enhanced coastal velocity in that region. Thus, although our model clearly supports faster spread in the western Mediterranean, we cannot conclude that this was the result of coastal leap-frog colonisation, rather than another directed mechanism with a similar outcome. Similarly, although both effects described above are quite different from a locally enhanced global propagation speed, our model would have difficulty (in a situation where the front was travelling along a coastline) in distinguishing the latter mechanism from an enhanced coastal velocity. We therefore also cannot rule out the possibility that the rapid spread along this coast was simply due to more rapid expansion favoured by low-intensity agriculture, as proposed by Bocquet-Appel *et al.* (2012). However, to explain our results, the latter effect would have to be dominated by agriculture within a coastal strip, similar to that used for our coastal velocity model.

If larger distance Lévy flight events are expected to be significant, they would have to be explicitly added to the underlying model, as they were for sea travel by Fort *et al.* (2012). Such events could be incorporated into our wavefront model, for example by the addition of stochastic steps ahead of the front (initiating secondary fronts, at least until subsequent re-mergers took place). Work in this direction would certainly be of interest, particularly in light of suggestions such as those of Collard *et al.* (2010) that the arrival of the Neolithic in the United Kingdom occurred via separate maritime routes, arriving independently in south-west England and in west-central Scotland. Sea travel is the most obvious phenomenon for which Lévy flights would seem to be appropriate; firmer archaeological evidence for the occurrence of large-scale travel events would be desirable before starting to model such flights on land.

There are, therefore, obvious ways in which our model needs to be developed further. Apart from the model refinements suggested by our results, the ^{14}C database needs to be extended to allow the finer details to be included in the model. However, the results presented here demonstrate the promise of such efforts, and offer a firm basis for further development towards advanced, qualitative understanding of the Neolithic dispersal and its interpretation in terms of human behaviour. In terms of specific mechanisms investigated here, our work confirms the importance of waterways and the enhanced mobilities that they allow in the spread of farming in the early Neolithic; it also takes the first steps towards robustly quantifying the extent to which this importance varied regionally with local environmental conditions.

Acknowledgements

This work was supported by the Leverhulme Trust under Research Grant F/00 125/AD.

References

AMMERMAN, A.J. & L.L. CAVALLI-SFORZA. 1971. Measuring the rate of spread of early farming in Europe. *Man* 6: 674–88. http://dx.doi.org/10.2307/2799190

BAGGALEY, A.W., R.J. BOYS, A. GOLIGHTLY, G.R. SARSON & A. SHUKUROV. 2012a. Inference for population dynamics in the Neolithic period. *Annals of Applied Statistics* 6: 1352–76. http://dx.doi.org/10.1214/12-AOAS579

BAGGALEY, A.W., G.R. SARSON, A. SHUKUROV, R.J. BOYS & A. GOLIGHTLY. 2012b. Bayesian inference for a wave-front model of the neolithization of Europe. *Physical Review E* 86: 016105. http://dx.doi.org/10.1103/PhysRevE.86.016105

BERNARDO, J.M. & A.F.M. SMITH. 1994. *Bayesian theory.* Chichester: Wiley. http://dx.doi.org/10.1002/9780470316870

BOCQUET-APPEL, J.-P., S. NAJI, M. VANDER LINDEN & J. KOZŁOWSKI. 2009. Detection of diffusion and contact zones of early farming in Europe from the space-time distribution of ^{14}C dates. *Journal of Archaeological Science* 36: 807–20. http://dx.doi.org/10.1016/j.jas.2008.11.004

—2012. Understanding the rates of expansion of the farming system in Europe. *Journal of Archaeological Science* 39: 531–46. http://dx.doi.org/10.1016/j.jas.2011.10.010

CLARK, J.G.D. 1965. Radiocarbon dating and the spread of farming economy. *Antiquity* 39: 45–48.

COLLARD, M., K. EDINBOROUGH, S. SHENNAN & M.G. THOMAS. 2010. Radiocarbon evidence indicates that migrants introduced farming to Britain. *Journal of Archaeological Science* 37: 866–70. http://dx.doi.org/10.1016/j.jas.2009.11.016

CZÁRÁN, T. 1998. *Spatiotemporal models of population and community dynamics*. London: Chapman & Hall.

DAVISON, K., P.M. DOLUKHANOV, G.R. SARSON & A. SHUKUROV. 2006. The role of waterways in the spread of the Neolithic. *Journal of Archaeological Science* 33: 641–52. http://dx.doi.org/10.1016/j.jas.2005.09.017

DOLUKHANOV, P., A. SHUKUROV, D. GRONENBORN, D. SOKOLOFF, V. TIMOFEEV & G. ZAITSEVA. 2005. The chronology of Neolithic dispersal in Central and Eastern Europe. *Journal of Archaeological Science* 32: 1441–58. http://dx.doi.org/10.1016/j.jas.2005.03.021

FORT, J. 2009. Mathematical models of the Neolithic transition: a review for non-mathematicians, in P. Dolukhanov, G. Sarson & A. Shukurov (ed.) *The East European Plain on the eve of agriculture* (British Archaeological Reports international series 1964). Oxford: Archaeopress.

FORT, J., T. PUJOL & M. VANDER LINDEN. 2012. Modelling the Neolithic transition in the Near East and Europe. *American Antiquity* 77: 203–19. http://dx.doi.org/10.7183/0002-7316.77.2.203

GAMMERMAN, D. & H. LOPES. 2006. *Markov chain Monte Carlo: stochastic simulation for Bayesian inference*. London: Taylor & Francis.

GANGAL, K., G.R. SARSON & A. SHUKUROV. 2014. The Near-Eastern roots of the Neolithic in South Asia. *PLoS ONE* 9: e95714. http://dx.doi.org/10.1371/journal.pone.0095714

GKIASTA, M., T. RUSSELL, S. SHENNAN & J. STEELE. 2003. Neolithic transition in Europe: the radiocarbon record revisited. *Antiquity* 77: 45–62.

HINZ, M., M. FURHOLT, J. MÜLLER, D. RAETZEL-FABIAN, C. RINNE, K.-G. SJÖGREN & H.-P. WOTZKA. 2012. RADON—radiocarbon dates online 2012. Central European database of ^{14}C dates for the Neolithic and Early Bronze Age. *Journal of Neolithic Archaeology* 14: 1–4.

ISERN, N. & J. FORT. 2010. Anisotropic dispersion, space competition and the slowdown of the Neolithic transition. *New Journal of Physics* 12: 123002. http://dx.doi.org/10.1088/1367-2630/12/12/123002

—2012. Modelling the effect of Mesolithic populations on the slowdown of the Neolithic transition. *Journal of Archaeological Science* 39: 3671–76. http://dx.doi.org/10.1016/j.jas.2012.06.027

Method

PRICE, T.D. 2003. The arrival of agriculture in Europe as seen from the north, in A.J. Ammerman & P. Biagi (ed.) *The widening harvest. The Neolithic transition in Europe: looking back, looking forward*: 273–94. Boston (MA): Archaeological Institute of America.

ROWLEY-CONWY, P. 2011. Westward ho! The spread of agriculture from Central Europe to the Atlantic. *Current Anthropology* 52: S431–S451. http://dx.doi.org/10.1086/658368

RUBIN, D.B. 1988. Using the SIR algorithm to simulate posterior distributions, in J.M. Bernardo, M.H. DeGroot, D.V. Lindley & A.F.M. Smith (ed.) *Bayesian statistics 3*: 395–402. Oxford: Oxford University Press.

STEELE, J. 2009. Human dispersals: mathematical models and the archaeological record. *Human Biology* 81: 121–40. http://dx.doi.org/10.3378/027.081.0302

ZILHÃO, J. 2001. Radiocarbon evidence for maritime pioneer colonization at the origins of farming in west Mediterranean Europe. *Proceedings of the National Academy of Sciences of the USA* 98: 14180–85. http://dx.doi.org/10.1073/pnas.241522898

—2003. The Neolithic transition in Portugal and the role of demic diffusion in the spread of agriculture across west Mediterranean Europe, in A.J. Ammerman & P. Biagi (ed.) *The widening harvest. The Neolithic transition in Europe: looking back, looking forward*: 207–23. Boston (MA): Archaeological Institute of America.

Received: 25 September 2013; Accepted: 12 December 2013; Revised: 16 June 2014